α_K's, the whole configuration can be described as a random matrix in which small ordered regions are distributed.

In conclusion, we note that the computer simulation of microstructure in disordered molecular crystals is very similar to that for binary alloys. These computations are expected to aid the theoretical calculation of diffuse scattering and will help in putting the data analysis on a better quantitative footing.

References

COWLEY, J. M. (1950). *J. Appl. Phys.* **21**, 24-30.

EPPERSON, J. E. (1979). *J. Appl. Cryst.* **12**, 351-356.

EPSTEIN, J. & WELBERRY, T. R. (1983). *Acta Cryst.* A**39**, 882-892.

GEHLEN, P. C. & COHEN, J. B. (1965). *Phys. Rev. A*, **139**, 844-855.

GRAGG, J. E. (1970). PhD thesis. Northwestern Univ., Evanston, IL, USA.

GRAGG, J. E., BARDHAN, P. & COHEN, J. B. (1971). *Critical Phenomena in Alloys, Magnets and Superconductors*, edited by R. E. MILLS, E. ASCHER & R. I. JAFFEE, pp. 309-337. New York: McGraw Hill.

KHANNA, R. & WELBERRY, T. R. (1987). *Acta Cryst.* A**43**, 718-727.

KHANNA, R. & WELBERRY, T. R. (1990). *Acta Cryst.* A**46**, 970-974.

KITAIGORODSKY, A. I. (1973). *Molecular Crystal and Molecules.* New York: Academic Press.

SIRIPITAYANANON, J. (1985). PhD thesis. Australian National Univ., Canberra, Australia.

WELBERRY, T. R., JONES, R. D. J. & EPSTEIN, J. (1982). *Acta Cryst.* B**38**, 1518-1525.

WELBERRY, T. R. & SIRIPITAYANANON, J. (1986). *Acta Cryst.* B**42**, 262-272.

WELBERRY, T. R. & SIRIPITAYANANON, J. (1987). *Acta Cryst.* B**43**, 97-106.

WILLIAMS, R. O. (1976). *ORFLS.* Report ORNL-TM-5140. Oak Ridge National Laboratory, Tennessee, USA.

WOOD, R. A., WELBERRY, T. R. & PUZA, M. (1984). *Acta Cryst.* C**40**, 1255-1260.

Acta Cryst. (1990). A**46**, 979-988

The Simulation of Condensed Phases in Cyclohexane Clusters

BY A. S. TREW, G. S. PAWLEY AND A. CAIRNS-SMITH†

Department of Physics, University of Edinburgh, King's Buildings, Mayfield Road, Edinburgh EH9 3JZ, Scotland

(*Received* 7 *May* 1990; *accepted* 23 *July* 1990)

Abstract

An extensive molecular dynamics study has been made as a prediction of possible structural phase changes in cyclohexane-d_{12}, using highly parallel computers. Clusters of 128 molecules and larger are simulated, giving results for zero-pressure conditions. Intermolecular interaction is modelled by 6-exp atom-atom potentials relating all non-bonded C and D atoms of rigid chair-form molecules. The system forms the natural low-temperature structure (phase II, space group $C2/c$), and on heating a transition is observed at 65 ± 10 K to a new rhombohedral phase (space group $R\bar{3}m$). This phase has not been found experimentally, but there is a natural unidentified metastable phase at ambient pressure and another unidentified phase under pressure. This new simulated phase persists to a further transition at 175 ± 15 K, above which there is no apparent molecular orientational ordering and the structure agrees well with the known f.c.c. plastic crystalline phase I. At 200 ± 15 K the plastic phase melts, and the liquid drop does not sublime, again in agreement with experiment. The analysis for the ordering in the clusters is done with the aid of equal area orientational and translational 'dot plots', radial distribution functions and powder diffraction patterns. Future bulk molecular dynamics simulations are suggested as a function of pressure, with the possible inclusion of the internal molecular distortion potential function.

1. Introduction

The development of molecular dynamics (MD) to model condensed systems goes back to the early work of Rahman (1964) and before. Considerable progress has since been made in the understanding of real systems through MD models, as evidenced by the work reported by Allen & Tildesley (1987), Tildesley (1987) and others. The use of MD to study the solid phases of matter is particularly appropriate for those systems whose phases are not highly ordered and crystalline. For the ordered systems, straightforward lattice-dynamical calculations give a good representation of the system behaviour, as reviewed by Pawley (1986); this is especially useful for those molecular systems where comparison with experiment is possible. For the more disordered systems one cannot use

† Deceased.

0108-7673/90/120979-10$03.00

the time-averaged unit cell as a good model and calculate its small vibrations, and therefore MD simulations have become the ideal way to set up models.

There are many examples of molecular systems in the solid state which are not crystalline, and they can mostly be classified as either liquid crystals or plastic crystals. The ordering that takes place in liquid crystals on cooling from the liquid phase is in the orientations of the molecules. These molecules are usually rather complex, and a realistic simulation of their behaviour is extremely computationally demanding. Somewhat less demanding is the simulation of plastic crystalline materials, reviewed by Sherwood (1979), where the ordering of the molecules below the liquid phase is translational and where a certain degree of orientational disorder characterizes the state. The shape of these molecules is rather spherical, and they are chemically simpler than the liquid-crystal molecules. Our aim is to perform as realistic a simulation as possible of a plastic crystalline solid and its solid-state phase transitions, especially if the results obtained can be used predictively.

Some success has already been achieved with some plastic crystals, ranging from the near-crystalline adamantane (Trew & Pawley, 1988) to the very plastic SF_6 (Fuchs & Pawley, 1988). A conclusion from both of these studies is that the plastic phase is perpetuated at a certain temperature by structural frustration which could not be explicitly built into the simulated model. This contrasts with work on *n*-butane (Refson & Pawley, 1987) where frustration does not seem to play such an important role and other determining structural mechanisms must be sought. The system chosen for study here is cyclohexane, known to have a plastic crystalline phase. A simplified model for this system has recently been studied by Schoen, Hoheisel & Beyer (1986), Hoheisel (1988) and Hoheisel & Würflinger (1989), but as the behaviour of such systems is often determined by the fine molecular structural details, we wish to study a rather more realistic model which will include all the atoms that comprise the molecule.

Cyclohexane has been studied extensively for a number of years, and its structures in the crystalline (II) and plastic (I) phases have been determined by Kahn, Fourme, André & Renaud (1973) (KFAR) by X-ray diffraction. Below the transition at 186·1 K found by Aston, Szasz & Finke (1943), phase II of cyclohexane is crystalline, space group $C2/c$, $a = 11{\cdot}23$, $b = 6{\cdot}44$, $c = 8{\cdot}20$ Å, $\beta = 108{\cdot}83°$ and $Z = 4$. Above the transition and below the melting point at 279·82 K phase I is plastic crystalline, $Fm3m$, $a = 8{\cdot}61$ Å. There have been many spectroscopic experimental studies on this system, especially as a function of temperature (Le Roy, 1965; Ito, 1965; Nevzorov & Sechkarev, 1971; Sataty & Ron, 1974; Rohrer, Falge & Brandmüller, 1978; Zhizhin, Krasyukov, Mukhtarov & Rogovoi, 1978; Mukhtarov, Rogovoi, Krasyukov & Zhizhin, 1979; Rogovoi & Zhizhin, 1980). The conclusions reached are consistent with the X-ray work except for the very early suggestion of Obremski, Brown & Lippincott (1968) that phase II was orthorhombic. The phase diagram becomes more complex when the effects of varying pressure are studied; two transitions have been found by Haines & Gilson (1989*a*) at room temperature at 0·51 and 0·96 GPa by infrared and Raman spectroscopy. The upper and lower phases are probably the same as I and II as found by KFAR, and the intermediate phase could well be orthorhombic. As there are many overlapping bands involving C–H stretching, the spectra are difficult to interpret, but Haines & Gilson (1989*b*) have recently obtained supportive evidence by using a dilute mixture of $C_6D_{11}H$ in cyclohexane-d_{12}. The effect of deuteration is to shift the two transitions to 0·53 and 0·74 GPa.

2. The MD model

Molecular dynamics simulations have been performed on clusters of perdeuterocyclohexane molecules, and three solid phases have been identified. The molecules have been assumed to be rigid, and fixed in the chair conformation, this being the most energetically favourable conformation with >99% concentration at room temperature (Carpenter & Halford, 1947). By assuming rigidity we neglect the energy contribution from the molecular distortion identified in the lowest phase in the X-ray work of KFAR, our argument for doing this being that this energy term should not be important in the higher-temperature phases where the molecular motion is less restricted. All the atom positions are included in the model molecule, unlike previous simulations, and the coordinates are given in Table 1. This molecule has bond lengths close to those of KFAR, but has idealized tetrahedrally bonded C atoms. It can be rotated into close coincidence with that found by the X-ray study, using two quaternions

$$Q_1 = (q_0; q_1, q_2, q_3)$$
$$= (0{\cdot}6526; -0{\cdot}1560, -0{\cdot}0037, 0{\cdot}7415)$$
$$Q_2 = (q_2; -q_3, -q_0, q_1)$$
$$= (-0{\cdot}0037; -0{\cdot}7415, -0{\cdot}6526, -0{\cdot}1560).$$

The components of these quaternions show the symmetry relation, and are expressed for orthogonal axes X, Y, Z in the crystal, X and Y along the monoclinic x and y axes, and z along z^*, perpendicular to x and y. Quaternions are now generally recognised as the best way to represent molecular orientations especially for simulations, as they do not have the pathological properties which make Euler angles inconvenient (Du Val, 1964; Evans, 1977; Pawley & Dove, 1985).

Table 1. *Atom positions* (Å) *for half a cyclohexane molecule relative to orthogonal axes*

The remaining coordinates are the same but with reversed signs.

	x	y	z
C	1·266	0·731	−0·258
C	1·266	−0·731	0·258
C	0·000	1·462	0·258
D	1·266	0·731	−1·231
D	1·266	−0·731	1·231
D	0·000	1·462	1·231
D	2·061	1·190	0·066
D	2·061	−1·190	−0·066
D	0·000	2·380	−0·066

The interaction potential is taken as the sum of all non-bonded atom–atom potentials, using the 6-exp potential of Kitaigorodskii (1966)

$$V_n(r) = -A_n/r^6 + B_n \exp(-\alpha_n r)$$

where r is the distance between a non-bonded pair, and n indicates the chemical pairing. The coefficients used for this work are those derived by Williams (1966, 1967), chosen because these values gave the best fit to phonon spectra. The units used here are as in the original papers, r in Å and V in kcal mol^{-1}.

		A_n	B_n	α_n
	C–C	568	83630	3·60
n:	C–H	125	8766	3·67
	H–H	27·3	2654	3·74

Although this potential has been optimized for hydrogenous molecules, we use it unaltered for perdeuterocyclohexane, choosing to model this form of the molecule as it is the deuterated form which is best for future coherent neutron scattering experiments. The structural changes on deuteration are expected to be small, following the electron diffraction experiment results of Ewbank, Kirsch & Schafer (1976), which show that the C–C bonds are unaltered but the C–H bond is about 0·007 Å longer than C–D, this being only marginally above experimental error. For this reason the mean C–H distance from KFAR has been slightly reduced.

We choose to simulate a cluster formed from a number of molecules and suspended in free space. Initially a spherical cluster is carved from bulk material, and it retains its spherical shape as monitored by the cluster inertia tensor. Cluster simulation has already been shown to be successful in modelling the solid–solid transition in SF_6 (Fuchs & Pawley, 1988), and the advantage in having free boundaries outweighs the disadvantage. The disadvantage is that a proportion of the molecules is involved in the surface of the cluster and therefore will not take up the bulk structure, and the MD sample must thus be sufficiently large for bulk properties to be observable in the interior. The advantage is that there is no unphysical constraint on the sample as experienced with cyclic boundary conditions, which for small systems either inhibit or force structural changes; for a MD sample that is large enough, a new phase can, however, grow in a polycrystalline form under these conditions (Pawley & Thomas, 1982). The size of cluster that we have found sufficient for detailed study is 128 molecules, having tested to ascertain that the same results are achieved with clusters of 256 molecules.

The simulation of clusters has been reviewed by Van de Waal (1983), but the method has not been extensively used to search for bulk properties in the solid. This review cites examples of atomic clusters which take on ordered (icosahedral) structures not occurring in the bulk, but such peculiarities have yet to be discovered in molecular systems, and the evidence from Fuchs & Pawley (1988) is that bulk property phenomena are repeated in the cluster. Nevertheless, because the quantity of bulk material is restricted, the bulk phenomena may not be exactly reproduced, and our simulations must be ultimately judged as models for clusters which can be produced experimentally. The free cluster method then gives the extra chance of studying almost any defect phenomenon, impurities, vacancies, interstitials, twinning, grain boundaries, surface effects. Phonons with both pressure and temperature effects must however be studied using the constant-pressure cyclic boundary technique of Parrinello & Rahman (1980), as has been done with some success for *n*-butane (Refson & Pawley, 1987).

Molecular dynamics uses the potential function for all the interacting molecules to find the instantaneous forces and torques required for solving Newton's equations. The positional and quaternion coordinates are time-stepped using the Beeman (1976) algorithm, which is accurate to the same level of approximation as the more commonly used Verlet (1968) algorithm. This gives good energy stability in our simulations, provided the time step is not too large. For all of this work, except immediately after initialization, we have used a time step of 0·015 ps. The energy fluctuation is then typically one part in 10^6 or 10^7 per step. This is close to the precision expected from arithmetic round-off in performing the calculations.

On initialization, or after a temperature change, it is necessary to let the cluster equilibrate. This is done as is usual by scaling all the velocity coordinates, which is equivalent to placing the system in a heat bath at the desired temperature. However, considerably more control must be used if this is to be treated as non-equilibrium MD. Equilibration is quite rapid in such an anharmonic system as cyclohexane; it usually takes from 20 to 40 ps to equilibrate as indicated by the potential energy becoming stable.

3. Computational method

Realistic MD simulations are very computationally demanding, and as they lend themselves well to the

exploitation of parallel computation they have benefited much from the recent development of this technology. Our study was started on the ICL DAP (Distributed Array Processor), designed in 1973 and operational in 1980 (Gostick, 1979; Hockney & Jesshope, 1981). This computer had 4096 processing elements (PEs), and the program was easily generalized for use on our more modern DAP 510 from AMT (Active Memory Technology) which has 1024 PEs. This machine is extremely cost-effective for this type of problem as all the processors can be kept working for all of the time.

The cluster simulations do not require a mapping of the system onto the computer as is done with the single-crystal simulations cited above where cyclic boundary conditions are invoked. Instead a simple use is made of the 'vector' and 'matrix' facilities on the DAP, now described. The PEs of the DAP 510 form a 32×32 array, and any variable which spans this array is called a 'matrix'. The rows or columns of the matrix are examples of 32-component 'vectors'. For the simulation of a 128-molecule cluster, the necessary data (one data set could be the x coordinates of the molecular centres of gravity) can be stored in sets of four vectors ($4 \times 32 = 128$). The information in one vector can be spread over a matrix such that all the rows of the matrix are identical. It is also possible to spread the vector of information over the matrix as columns, and by combining these two procedures the elements of the matrix itself can be used for the interaction between the molecules represented by the elements of the row vectors and those represented by the elements of the column vectors. As the information is contained in vector sets (four in each for this 128-molecule example), the full interaction has to be calculated serially over the constituent vectors. A little care is needed when the same vector set of molecules is used for both the row and the column vectors as the interaction is then calculated twice and the matrix diagonal must be ignored. This represents a loss of efficiency which could be redeemed by some intricate programming, but we consider this not to be worthwhile as the loss is only 20% for the 128-molecule cluster, and would be less for a larger cluster.

This method of computation has its major inefficiency in the calculation of interactions between distant molecules, which could otherwise be ignored. This is one of the penalties of SIMD (single instruction multiple data) computation, where each PE has to do the same operation as all the others at any one time or remain idle. This can be avoided in serial or MIMD computers at the expense of organizing interaction neighbour lists. There are of course other strategies that could be employed for SIMD computers to make them more efficient on bigger systems, such as domain decomposition, but this has not been found necessary for the systems we discuss here.

One of the strengths of the DAP is its wide internal bandwidth, which allows global summations to be done very efficiently. Thus in the present problem, when all the intermolecular forces have been calculated at the elements of matrices, they can be summed along the rows or down the columns to give the total forces required for a time step. The inefficiencies of the simple algorithm outlined above are thus offset to a certain degree by the special SIMD architecture facilities. This balance is typical of parallel computers of various architectures, and makes comparisons of different machines rather difficult. However it is most likely that the large MD simulations of the future will be done increasingly on highly parallel computers.

4. Analysis

We have developed two basic methods for the analysis of the simulated clusters, an 'orientational analysis' and a 'structural analysis'. Both are based on the construction of the 'dot plot', which will be described in the next paragraph. Analysis difficulties arise because there are no fixed directions in a cluster sample as there are for a cyclically bound crystal, nor is there a reliable translational periodicity. This makes the construction of order parameters rather difficult, and the behaviour is best represented diagramatically.

The orientational dot plot is designed to display any ordering of the molecular orientations that take place. In the chair conformation a cyclohexane molecule has trigonal symmetry, and it is possible to choose four directions which adequately specify its orientation. One of these vectors is perpendicular to the mean plane through the six carbon atoms, and the other three lie in that plane along the molecular diad axes. If we project these four vectors in both the positive and negative directions from the centre of the molecule to intersect a very large sphere centred on the cluster, the eight points of intersection fully characterize the orientation. All those molecules of similar orientation then produce a grouping of intersection points on the sphere. Because the molecules are centrosymmetric, all the orientational information is contained in one hemisphere. Each molecule will give rise to four intersections in the chosen hemisphere, and these can be projected on to the equatorial plane by the equal area projection. (This is the Lambert azimuthal equivalent projection, where the distance from the pole to an intersection point on the hemisphere along a straight line is used as the radius for the projected point on the equatorial plane, positioned at the same azimuthal angle.) The density of points (dots) on the plot thus corresponds exactly to the solid angle density of the orientational distribution function, and this we call the orientational dot plot. Furthermore, the spread of points in a peak in the dot plot gives a good indication of the mean thermal motion.

The structural dot plot is designed to show translational ordering, and can be constructed along with the modified RDF, the radial distribution function; the modification here is the reduction of the more distant contributions to the usual RDF because the cluster system is finite. While calculating the distances for the RDF, those which correspond to close neighbour vectors can be sorted out, and the vectors themselves used to construct a dot plot. Again only a hemisphere needs to be projected as the distribution of vectors is clearly centrosymmetric. The grouping of the dots on such a dot plot is a very sensitive test for translational ordering, and the RDF can be used to obtain the lattice parameters. We prefer to use the RDF for this, rather than to calculate lattice parameters from powder diffraction patterns, because such calculations are computationally intensive and the small size of the cluster (radius about 20 Å) means that any features in the Fourier transform are very broad. It is consequently difficult to measure lattice spacings accurately in this way, whereas they can be measured to about ±0·1 Å from the RDF.

4.1. *The C2/c phase*

In this phase the primitive crystal unit cell contains two molecules, their orientations being related by the *c*-glide symmetry operation; this is the relationship between the two quaternions given earlier. KFAR give the angle between the normal to the best plane through the C atoms of the molecule and the *c* axis as 13·3°, though our estimate from their published values is 12·1°; we will call this the Kahn angle. In terms of the model quaternion values given above, a Kahn angle of 11·42° is readily found from

$$0{\cdot}5\cos^{-1}[16q_1q_2q_3q_0+q_1^4+q_2^4+q_3^4+q_0^4 +2(q_1^2q_2^2+q_1^2q_3^2+q_0^2q_2^2+q_0^2q_3^2) -6(q_0^2q_1^2+q_2^2q_3^2)].$$

A cluster was set up in this phase with lattice parameters as determined experimentally at 115 K. After equilibration at 10 K, only a slight relaxation of the system was observed which resulted in a reduction of the lattice parameters by about 0·1 Å, and a change of the Kahn angle to 12·5°.

A section through the fully equilibrated cluster at 10 K shown in Fig. 1, parallel to the crystallographic *ab* plane, with the *a* axis across the page. Three numbered layers of molecules are shown in C skeletal form, with three C atoms specially identified in each molecule. This serves to identify the *c*-glide symmetry operation first from a molecule at level 1 to level 2 and then back to level 3.

Figs. 2(*a*) and (*b*) show the orientational and translational dot plots for this cluster. Near the centre of Fig. 2(*a*) there are the two peaks corresponding to the molecular triad axes, separated by twice the Kahn angle. The great circles for which these two peaks are poles clearly contain the sets of diad axis peaks. These diagrams have additional value when the various molecular axes are represented by different colours, as they then show when molecules have undergone a 120° rotation about the triad axis. Such motion is not expected until temperatures of above 150 K are reached, according to the NMR experiments of Andrew & Eades (1953). Examination of Fig. 2(*b*) shows six vector peaks in the equatorial plane at roughly 60° intervals, in agreement with the X-ray structural work which shows the angle between **b** and (**a**+**b**)/2 differing from 60° by only $\delta = 0{\cdot}17°$, where

$$\delta = (a - 3^{1/2}b)/4b.$$

The three different lattice spacings that these peaks represent are described in terms of their $\langle n_1, n_2, n_3\rangle$ triplets as ⟨0, 2, 0⟩ and ⟨1, ±1, 0⟩, the translations being

$$n_1\mathbf{a}/2 + n_2\mathbf{b}/2 + n_3\mathbf{c}/2.$$

The peaks in the body of the diagram are arranged as follows, the · symbols representing the equatorial peaks.

·⟨0, −2, 0⟩
⟨1, −2, 1⟩
·⟨−1, −1, 0⟩ ⟨0, −1, 1⟩ ·⟨1, −1, 0⟩
⟨1, −1, 2⟩
⟨−1, 0, 1⟩ ⟨0, 0,2⟩ ⟨1, 0, 1⟩
⟨1, 1, 2⟩
·⟨−1, 1, 0⟩ ⟨0, 1, 1⟩ ·⟨1, 1, 0⟩
⟨1, 2, 1⟩
·⟨0, 2, 0⟩

The spread in the equatorial peaks gives a good

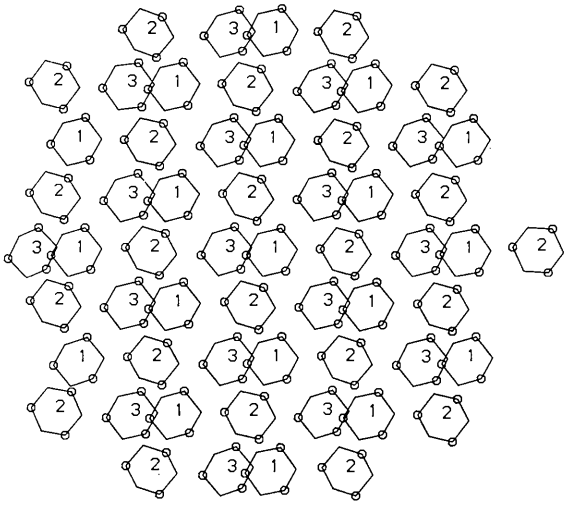

Fig. 1. A section through the cluster at 10 K, parallel to the crystallographic *ab* plane, with the *a* axis across the page. Molecules on three *z* levels are shown, numbered 1, 2 and 3. Only the C skeleton is shown, and three C atoms are identified in each molecule. This identification relates molecules numbered 1 and 3 to those numbered 2 by the *c*-glide symmetry operation.

indication of the limit in accuracy in determining interaxial angles from these diagrams.

The main purpose of the dot plots is searching for order in the clusters, as they cannot be compared directly with experiment. However, experiment does yield electron diffraction patterns from cluster jets, as shown for SF_6 by Farges, de Feraudy, Raoult & Torchet (1985). We present in Fig. 3(*a*) the diffraction patterns expected from the various cyclohexane phases found at a number of temperatures, calculated by the standard method from the radial distribution function as described recently by Bartell (1986). The $C2/c$ phase is characterized by the plot at the lowest temperature, and this persists to 50 K. By 75 K the diffraction pattern has changed markedly and a phase transition has clearly taken place.

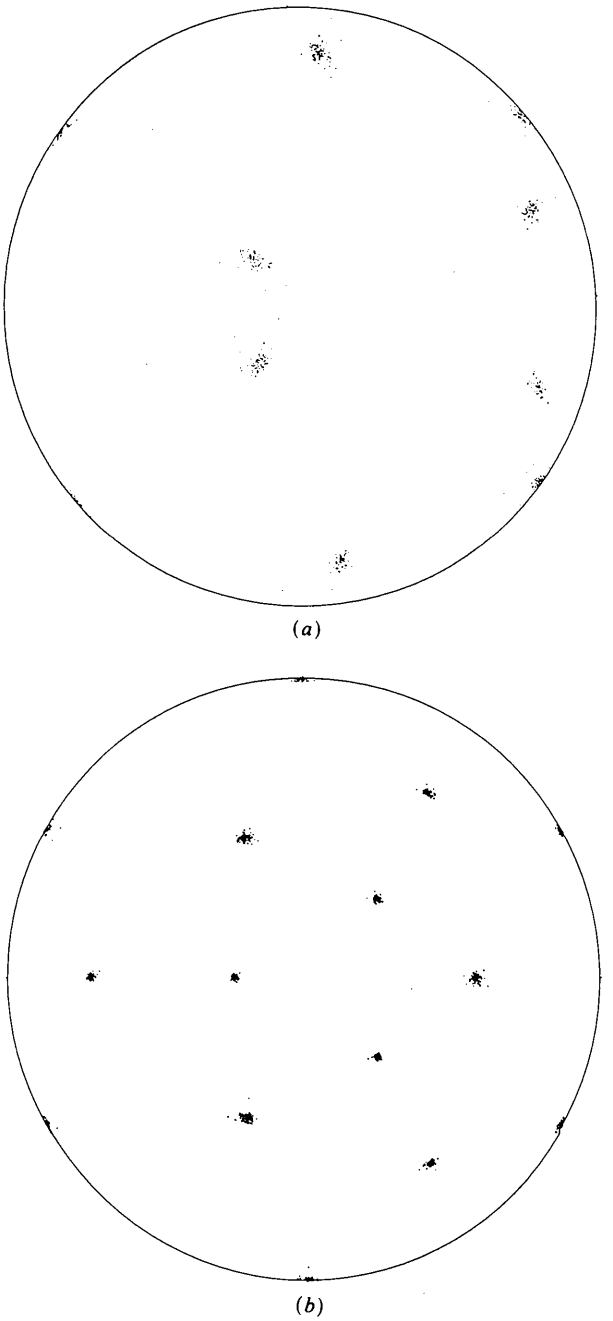

(*a*)

(*b*)

Fig. 2. Dot plots showing (*a*) the orientational distribution function and (*b*) the translational distribution function for distances up to 9 Å, for cyclohexane-d_{12} at 10 K. Note that in (*b*) the more distant peaks, identified in the text, appear more concentrated.

4.2. *The new rhombohedral phase*

On heating the cluster a transition was observed at 65 ± 10 K to a new phase. This is well below the expected temperature of 186·1 K for the transition to the plastic phase, but transitions could well take place at lower temperatures in clusters than in the bulk because of the increased surface-to-volume ratio. However, the transition observed is not the plastic transition, and therefore we must investigate the new structure in some detail.

Fig. 4 shows a section of three planes of molecules in the cluster after equilibration at 75 K, similar to Fig. 1. All the molecules in the central region of the cluster have now become oriented with their triad axes perpendicular to the plane of the diagram, though there are now more molecules in disturbed orientations near the surface owing to the increased thermal motion. The orientational dot plot of Fig. 5(*a*) confirms the change to one molecular orienta-

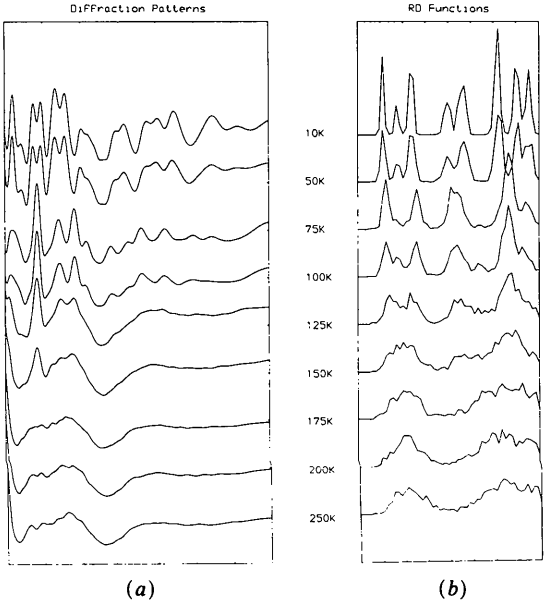

(*a*) (*b*)

Fig. 3. (*a*) Cluster diffraction patterns at 10, 50, 75, 100, 125, 150, 175, 200 and 250 K, for 128-molecule clusters; a wavelength $\lambda = 1{\cdot}6$ Å is used, and 2θ varies from 0 to 160°. (*b*) Radial distribution functions (RDFs) for molecule centre distances calculated for the same temperatures; the figure spans from 4 to 12 Å. These temperatures span both solid–solid phase transitions and melting.

tion, and it is clear from the spread of points in the translational dot plot of Fig. 5(*b*) that it is not possible to measure δ as different from zero, using the peaks in the equatorial plane of Fig. 5(*b*). Thus the Kahn angle has gone to zero, and the interaxial discrepancy of $\delta = 0{\cdot}17°$ noted above for the $C2/c$ structure has vanished.

The powder diffraction patterns for this phase at temperatures 75, 100, 125 and 150 K are given in Fig. 3(*a*). Comparison of the diffraction patterns at 50 and 75 K show that the latter has lost much of the structure visible in the former, indicating a more symmetric crystal structure. Measurement of angles around the great circles of Fig. 5(*b*) between the three peaks in the central region of the figure gives 77·5 (5), 78·2 (5) and 78·2 (5)°. All this evidence points to a rhombohedral space group with $\alpha = 78{\cdot}0°$. The extra symmetry that appears in this phase is not the result of a stochastic average, and thus this rhombohedral phase is a true crystalline phase. Its space group is $R\bar{3}m$. From the RDFs of Fig. 3(*b*) we see that, at 75 K, $a = 5{\cdot}25$ (10) Å.

Further heating of the cluster to 100 K showed a tendency for the lattice parameter to increase marginally to 5·3 Å and the lattice angle to fall to 77°. This trend became more obvious at higher temperatures, as shown in Table 2. The reduction in α is interesting as it implies that the structure is approaching cubic symmetry. In a f.c.c. lattice there is an angle of 60° between the vectors [110], [101] and [011], these being the cell vectors of the primitive rhombohedral cell with trigonal axis along the cube [111], and it is clear from Table 2 that at 175 K the simulation structure has in fact relaxed to f.c.c. symmetry. From Fig. 3(*a*) it would appear that the cubic phase has been reached, as the diffraction patterns contain no dominant peaks at this temperature.

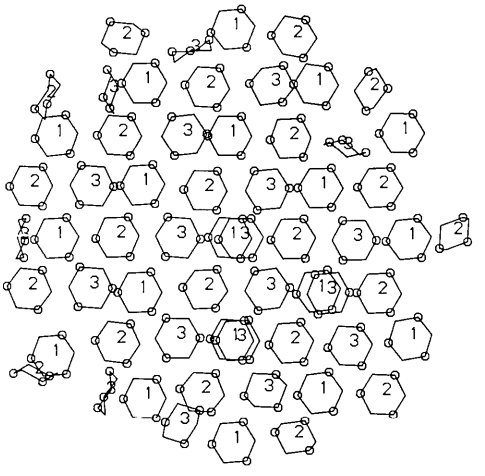

Fig. 4. A section through the cluster at 100 K, similar in detail to Fig. 1. The molecules are now aligned with their trigonal axes perpendicular to this plane, and a diad axis along the *b* axis (up the page).

Before considering the plastic phase, let us investigate whether the rhombohedral phase could exist and have been missed in the X-ray work. It could in fact be the metastable phase III reported by KFAR which annealed to phase II ($C2/c$ phase) between 120 and 186 K. As phase III is obtained by quick cooling it is possible that in the non-equilibrium process there is considerable orientational thermal disorder about

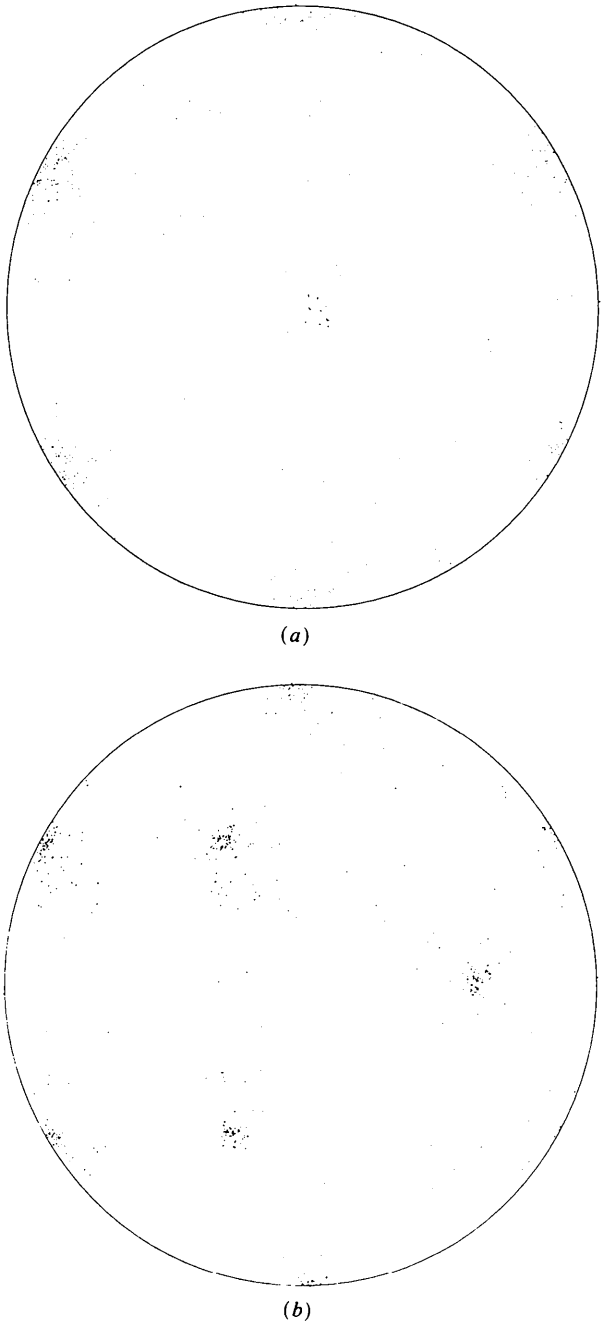

(*a*)

(*b*)

Fig. 5. Dot plots showing (*a*) the orientational distribution function and (*b*) the translational distribution function at 100 K; (*b*) differs from Fig. 2(*b*) by having vectors only up to 7 Å, giving nearest-neighbour vectors only.

Table 2. *The temperature dependence of the rhombohedral cell constants*

T(K)	a(Å)	α(°)
75	5·25 (10)	78 (1)
100	5·30 (10)	77 (1)
125	5·45 (15)	70 (1)
150	5·7 (3)	68 (2)
165	5·8 (3)	64 (3)
175	6·0 (3)	60 (3)

the molecular trigonal axes, making the rhombohedral structure preferable. On annealing, this structure suffers a shearing motion and phase II becomes stabilized by the molecular distortion identified by KFAR as small but significant.

We can understand the shear distortion from the translational dot plots of Figs. 2(b) and 5(b) and Fig. 6. The three largest peaks in Fig. 2(b) correspond to the shortest lattice vectors out of the ab plane.

$$\langle 0, -1, 1\rangle \qquad \langle 1, 0, 1\rangle$$

$$\langle 0, 1, 1\rangle$$

These become the rhombohedral cell edges, and by adding them together we get the cell body diagonal along the trigonal axis, $\langle 1, 0, 3\rangle \equiv (\mathbf{a}+3\mathbf{c})/2$. On shearing to the rhombohedral structure these three shortest vectors become trigonally symmetric about the centre, as seen in Fig. 5(b) where a 7 Å cut off is used. The shearing can be understood from Fig. 6, which shows C-skeletal molecules projected on the ac plane, $C2/c$ structure. The shear distortion is characterized by

$$\varepsilon = (a + 3c\cos\beta)/2$$

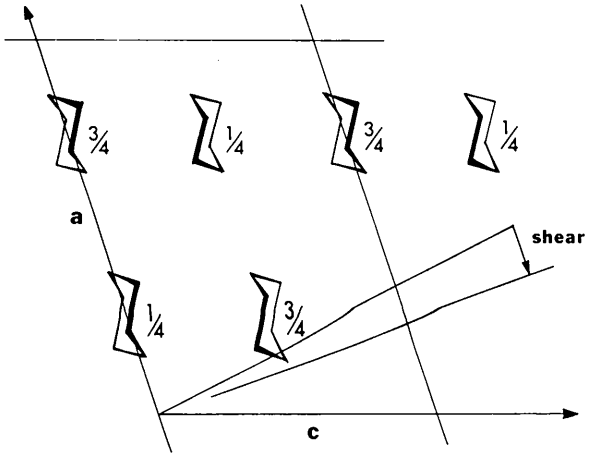

Fig. 6. Schematic drawing of the $C2/c$ structure from Kahn *et al.* (1973), projected down the b axis. The molecules are clearly tilted out of the ab plane (hence the 'Kahn' angle). The planes of molecules have to shear as shown to move into the simulated rhombohedral structure, and the molecules must reorient into the ab plane. An expression for the shear length ε is given in the text.

and by δ defined earlier. The transition requires that both δ and ε must go to zero along with the Kahn angle. We have performed neutron powder diffraction experiments, and have not found evidence of the existence of this phase at ambient pressure.

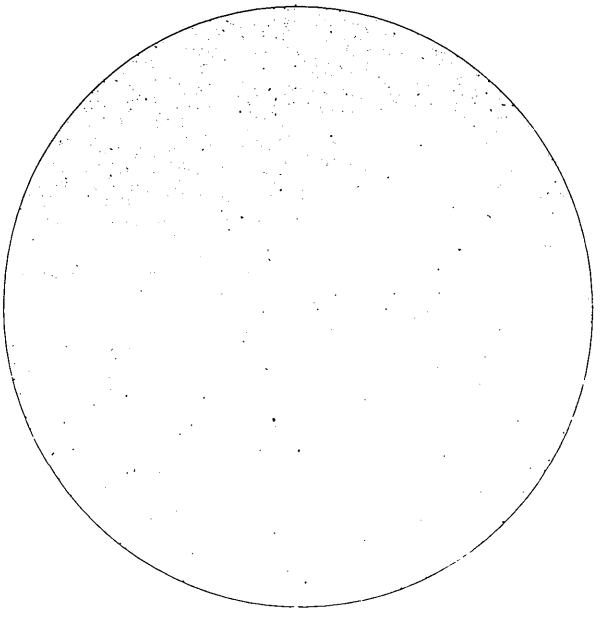

(a)

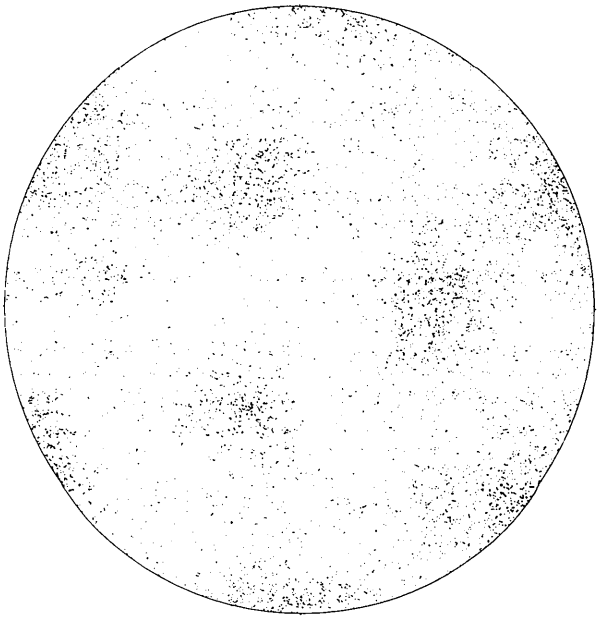

(b)

Fig. 7. Dot plots showing (a) the lack of orientational order and (b) the remaining translational order with a 7 Å nearest-neighbour vector length limit, in the cluster at 175 K. Unlike the other dot plots presented here, these are a superposition of a number of distributions taken over an extended period of time, as a single snapshot gives no indication of ordering.

4.3. *The f.c.c. phase*

The reduction of the rhombohedral α to 60° as shown in Table 2 indicates that the structure is now f.c.c., a (cubic) = 8·5 (4) Å [$=2^{1/2}a$(rhomb.)], with random molecular orientations, having transformed at 175 ± 15 K. This is in good agreement with the experimentally observed plastic phase, for which the transition temperature is 186·1 K and the unit-cell length is $a = 8{\cdot}61$ Å. Translational ordering is retained in the cluster through this transition, but this we can deduce only from the dot plots and section diagrams.

The lack of orientational order at 175 K is shown by Fig. 7(a); no peaking is observed in this diagram (nor was any apparent in the working diagrams where the triad and diad axes were colour coded). Nevertheless there is translational order as the dot plot in Fig. 7(b) shows. A cross section similar to Fig. 1 is given in Fig. 8; this has to be looked at with care to discern the translational ordering, but this can be seen by concentrating attention on the molecules labelled with the same z-height number.

4.4. *Melting*

At temperatures of 200 K and above the translational and orientational dot plots show no order, indicating that the sample has melted. This is supported by autocorrelation functions which show that the molecules at 200 K undergo diffusion. That the cluster melts rather than sublimes is again consistent with the behaviour of the natural material.

The melting point of the natural material is 279·82 K, and in this regard the present model seems to be lacking. However, we propose that the inaccuracies that are introduced by the fact that the simulation is of a cluster will be most at the higher temperatures, where surface effects will penetrate more. Simulations of other clusters have indicated that there is a drop in phase change temperatures, especially at higher temperatures, dropping even further as the cluster size is reduced. Shorter runs on larger clusters do indicate that the same phenomena are observable, but to get a better estimate of the melting temperature in this model system we would have to perform more extensive simulations on larger clusters.

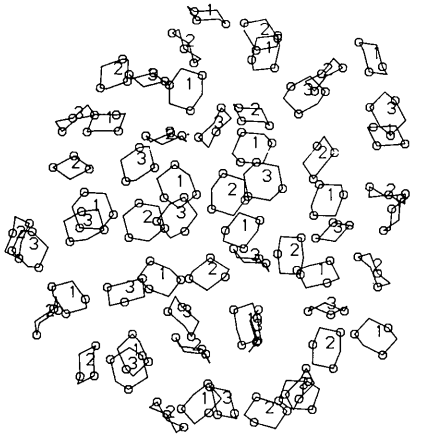

Fig. 8. A cross section through the cluster at 175 K, similar to Fig. 1, in which the translational ordering can be discerned by concentrating attention on the positions of the molecules marked with the same z-coordinate number.

5. Concluding remarks

A comprehensive MD study has been made of the structural phase changes in clusters of cyclohexane-d_{12}. The main results recorded were obtained with clusters of 128 molecules, but some simulations of larger clusters have shown similar phenomena, suggesting that the surface free energy is not the driving force for the observed transitions. The system gave a phase structure very similar to that of the natural material, except that an intermediate rhombohedral phase was found. This could be the metastable phase mentioned by KFAR. Alternatively it could be the new phase which appears when pressure is applied to the natural material as studied by Haines & Gilson (1989a, b), though this is thought to be orthorhombic. It would therefore be interesting to undertake a MD study of the bulk so that pressure could be applied, but it might be necessary to include the internal distortion of the molecules as this is believed by KFAR to be important in phase II and could well be more important under pressure. MD is becoming a tool for structure prediction, and we hope that this simulation will lead to further experimental studies.

We thank the Science and Engineering Research Council UK for its support of one of us (AST) and of the two ICL DAPs in Edinburgh, and to the Alvey Committee for its support of the AMT DAP 510-4 under project ARCH001. Moreover we are grateful to SERC for the research studentship for Adam Cairns-Smith before his most untimely death, and especially to Dr Peter Hatton who initiated the project and has contributed much to it.

References

ALLEN, M. P. & TILDESLEY, D. J. (1987). *Computer Simulation of Liquids.* Oxford Univ. Press.

ANDREW, E. R. & EADES, R. G. (1953). *Proc. R. Soc. London Ser. A*, **216**, 398-412.

ASTON, J. G., SZASZ, G. J. & FINKE, H. L. (1943). *J. Am. Chem. Soc.* **65**, 1135-1139.

BARTELL, L. S. (1986). *Chem. Rev.* **86**, 491-505.

BEEMAN, D. (1976). *J. Comput. Phys.* **20**, 130-139.

CARPENTER, G. B. & HALFORD, R. S. (1947). *J. Chem. Phys.* **15**, 99-106.

DU VAL, P. (1964). *Homographies, Quaternions and Rotations.* Oxford Univ. Press.

EVANS, D. J. (1977). *Mol. Phys.* **34**, 317-323.

EWBANK, J. D., KIRSCH, G. & SCHAFER, L. (1976). *J. Mol. Struct.* **31**, 39-45.
FARGES, J., DE FERAUDY, M. F., RAOULT, B. & TORCHET, G. (1985). *Surf. Sci.* **156**, 444-450.
FUCHS, A. H. & PAWLEY, G. S. (1988). *J. Phys. (Paris)*, **49**, 41-51.
GOSTICK, H. (1979). *ICL Tech. J.* **1**, 116-135.
HAINES, J. & GILSON, D. F. R. (1989*a*). *J. Phys. Chem.* **93**, 20-23.
HAINES, J. & GILSON, D. F. R. (1989*b*). *J. Phys. Chem.* **93**, 7920-7925.
HOCKNEY, R. W. & JESSHOPE, C. R. (1981). *Parallel Computers.* Bristol: Adam Hilger.
HOHEISEL, C. (1988). *J. Chem. Phys.* **89**, 3195-3202.
HOHEISEL, C. & WÜRFLINGER, A. (1989). *J. Chem. Phys.* **91**, 473-476.
ITO, M. (1965). *Spectrosc. Acta*, **21**, 2063-2076.
KAHN, R., R. FOURME, R., ANDRÉ, D. & RENAUD, M. (1973). *Acta Cryst.* **B29**, 131-138.
KITAIGORODSKII, A. I. (1966). *J. Chim. Phys.* **63**, 9-16.
LE ROY, A. (1965). *C. R. Acad. Sci. Ser. B*, **260**, 6079-6082.
MUKHTAROV, E. I., ROGOVOI, V. N., KRASYUKOV, YU. N. & ZHIZHIN, G. N. (1979). *Opt. Spektrosk.* **46**, 920-925.
NEVZOROV, B. P. & SECHKAREV, A. V. (1971). *Izv. Vuz. Fiz.* **2**, 75-83.
OBREMSKI, R. J., BROWN, C. W. & LIPPINCOTT, E. R. (1968). *J. Chem. Phys.* **48**, 185-191.
PARRINELLO, M. & RAHMAN, A. (1980). *Phys. Rev. Lett.* **45**, 1196-1199.
PAWLEY, G. S. (1986). In *Neutron Scattering*, edited by D. L. PRICE & K. SKOLD. New York: Academic Press.
PAWLEY, G. S. & DOVE, M. T. (1985). *Mol. Phys.* **55**, 1147-1157.
PAWLEY, G. S. & THOMAS, G. W. (1982). *Phys. Rev. Lett.* **48**, 410-413.
RAHMAN, A. (1964). *Phys. Rev.* **136A**, 405-411.
REFSON, K. & PAWLEY, G. S. (1987). *Mol. Phys.* **61**, 669-692, 693-709.
ROGOVOI, V. N. & ZHIZHIN, G. N. (1980). *Fiz. Tverd. Tela*, **17**, 376.
ROHRER, U., FALGE, H. J. & BRANDMÜLLER, J. (1978). *J. Raman Spectrosc.* **7**, 15-17.
SATATY, Y. A. & RON, A. (1974). *Chem. Phys. Lett.* **25**, 384-386.
SCHOEN, M., HOHEISEL, C. & BEYER, O. (1986). *Mol. Phys.* **58**, 699-709.
SHERWOOD, J. N. (1979). *The Plastic Crystalline State.* New York: Wiley.
TILDESLEY, D. J. (1987). *Computational Physics*, edited by R. D. KENWAY & G. S. PAWLEY, pp. 52-105. Edinburgh Univ. Press.
TREW, A. S. & PAWLEY, G. S. (1988). *Can. J. Chem.* **66**, 1018-1025.
VAN DE WAAL, B. W. (1983). *J. Chem. Phys.* **79**, 3948-3961.
VERLET, L. (1968). *Phys. Rev.* **165**, 201-214.
WILLIAMS, D. E. (1966). *J. Chem. Phys.* **45**, 3770-3778.
WILLIAMS, D. E. (1967). *J. Chem. Phys.* **47**, 4680-4684.
ZHIZHIN, G. N., KRASYUKOV, YU. N., MUKHTAROV, E. I. & ROGOVOI, V. N. (1978). *Pis'ma Zh. Exp. Teor. Fiz.* **28**, 465-468.

Acta Cryst. (1990). A**46**, 988-992

Phase Determination and Patterson Maps from Multiwavelength Powder Data

BY W. PRANDL

Institut für Kristallographie, Universität Tübingen, Charlottenstrasse 33, *D*-7400 *Tübingen, Federal Republic of Germany*

(*Received* 30 *April* 1990; *accepted* 24 *July* 1990)

Dedicated to Professor K. Fischer on the occasion of his 65th birthday.

Abstract

In the limit of unrestricted resolution, with Friedel pairs as the only coincidences, phase angles or signs can be determined uniquely from powder diffraction data using multiple-wavelength techniques. For a centrosymmetric structure one anomalously scattering species of atoms and data taken at two λ's are sufficient. In the acentric case one needs two different anomalous scatterers and measurements at three λ's. The anomalous scatterers can be localized from difference Patterson maps: their peaks can be discriminated against the peaks due to non-anomalous scatterers.

I. Introduction

Anomalous scattering effects in X-ray powder data have been taken into account so far mostly as corrections of the form factor for the profile refinement, *e.g.* in the program by Young, Mackie & Von Dreele (1977). In a powder diagram reflections **H** and $-\mathbf{H}$ coincide exactly. Bijvoet differences as well as Bijvoet ratios can therefore not be determined from powder data, and so all methods of phase determination based on either quantity cannot be applied. Another practical restriction of the powder method at conventional X-ray sources has been the limited resolution which causes, in addition to the Friedel pairs, further coincidences. The availability of high-resolution powder diffractometers at synchrotron X-ray sources has improved the experimental situation in several respects:

(i) The resolution has been improved substantially above conventional diffractometers: line widths (FWHM) of $\Delta(2\theta) \leq 0{\cdot}025°$ in $30 \leq 2\theta \leq 80°$ have been reported by Wroblewski, Ihringer & Maichle (1988). Reinhardt (1989) found these line widths smaller by a factor $\simeq 5$ than corresponding values from a high-resolution Guinier diffractometer.

0108-7673/90/120988-05$03.00